

Final Draft
of the original manuscript:

Brokmeier, H.-T.; Gan, W.M.; Randau, C.; Voeller, M.; Rebelo-Kornmeier, J.; Hofmann, M.:

Texture analysis at neutron diffractometer STRESS-SPEC

In: Nuclear Instruments and Methods in Physics Research A (2011) Elsevier

DOI: 10.1016/j.nima.2011.04.008

Texture analysis at neutron diffractometer STRESS-SPEC

H.-G. Brokmeier ^{a, b}, W. M. Gan ^{b, *}, C. Randau ^a, M. Völler ^c, J. Rebelo-Kornmeier ^c, M. Hofmann ^c

^a Institute for Materials Science and Engineering, Clausthal University of Technology, D-38678 Clausthal-Zellerfeld, Germany

^b Institute of Materials Research, Helmholtz-Zentrum Geesthacht, out Station at FRM II, Lichtenbergstr. D-85747 Garching, Germany

^c FRM II, TU München, Lichtenbergstr. 1, D-85747 Garching, Germany

***Corresponding author,**

Post address: HZG out Station at FRM II, Lichtenbergstr. 1, D-85747 Garching, Germany

Tel: +49-8928910766; **Fax:** +49-8928910797

E-mail: weimin.gan@hzg.de

Abstract

In response to the development of new materials and the application of materials and components in advanced technologies, non-destructive measurement methods of textures and residual stresses have gained worldwide significance in recent years. The materials science neutron diffractometer STRESS-SPEC at FRM II (Garching, Germany) is designed to be applied equally to texture and residual stress analyses by virtue of its very flexible configuration. Due to the high penetration capabilities of neutrons and the high neutron flux of STRESS-SPEC it allows a combined analysis of global texture, local texture, strain pole figure and FWHM pole figure in a wide variety of materials including metals, alloys, composites, ceramics and geological materials. Especially, the analysis of texture gradients in bulk materials using neutron diffraction has advantages over laboratory X-rays and EBSD for many scientific cases. Moreover, neutron diffraction is favourable for coarse grained materials, where bulk information averaged over texture inhomogeneities is needed, and also stands out due to easy sample preparation. In future, the newly developed robot system for STRESS-SPEC will allow much more flexibility than an Eulerian cradle as on standard instruments. Five recent measurements are shown to demonstrate the wide range of possible texture applications at STRESS-SPEC diffractometer.

Keywords: neutron diffraction, texture analysis, robot technique, peak broadening pole figure

1. Introduction

Together with the microstructure, polycrystalline materials are characterised by their texture - the distribution function of the crystallographic orientations of grains in relation to the sample coordinate system. Quantitative texture analysis is therefore essential in the investigation of new materials, to study anisotropic behaviour and to optimise technological processes like deep drawing, bending, metal spinning, etc., in applied as well as in fundamental researches [1, 2]. Neutron diffraction method for texture analysis is similar to well-known X-ray diffraction techniques. The main advantage of neutron diffraction over X-ray diffraction, however, arises from the fact that the interaction of neutrons with material is relatively weak and it is not related to the number of electrons; and consequently the penetration depth of neutrons is up to 10^2 - 10^3 larger than that of laboratory X-ray diffraction [3, 4].

Nearly 30 years after the discovery of the neutron by Chadwick (1923) [5], the first neutron diffraction texture measurement was carried out by Brockhouse (1953) [6]. As a consequence of the behaviour of neutrons when interacting with material (see e.g. Bacon, [7]), neutron diffraction became an additional diffraction technique to X-ray or electron diffraction. Bunge [8] combined neutron texture measurements on Cu-sheet firstly with a newly developed quantitative texture described by the orientation distribution function (ODF) based on the harmonic method. Since that time neutron diffraction became a standard method in bulk texture analysis producing the highest quality ODF data compared to all other methods. Today, neutron diffraction is a standard method in a large variety of investigations in physical,

chemical, material, and geological science. Particularly, the interests in engineering based projects are increased strongly with improving experimental options.

With neutron diffraction bulk samples rather than surfaces are measured. Therefore, coarse-grained materials can be characterised easily; averaging over texture inhomogeneities of mechanical test samples can open the direct correlation between texture and material's properties. Moreover, environmental cells (heating, cooling and deformation, etc.) are available and the angular resolution in orientation space is better than for an X-ray pole figure goniometer because no defocusing occurs. It is also possible to measure complex multi-phase composites with many closely spaced diffraction peaks depending on instrumental resolution. In general, no additional surface treatments of the samples (like polishing) are necessary in neutron global texture measurements.

The step to local texture and non-destructive texture measurements of semi-finished products is related to instrumental improvements to increase the neutron flux, to improve the freedom in sample tilting and rotation; and to develop evaluation and correction procedures for incomplete pole figures, for variable scanning grids, for anisotropic absorption and variable gauge volumes. The materials science neutron diffractometer STRESS-SPEC at FRM-II was developed as a multi-purpose diffractometer for strain and crystallographic texture investigations to deal with these challenges. With a focus on stress evaluation a description of STRESS-SPEC was already given by Hofmann et al. [9-11]. The present paper will concentrate solely on texture analysis, giving five typical examples in deformed metals (an Al sheet) and local texture on a Mg extrusion profile with bonelike shape, multi-phase material (Al-Mg composite), geological sample (calcite), and an example of peak intensity, peak position and peak broadening pole figures.

2. Instrumental setup

The materials science neutron diffractometer STRESS-SPEC is located at a thermal beam port and comprises a highly flexible monochromator arrangement, utilizing three different monochromators. To combine the need for pole figure and precise d-value determination the monochromator take off angle can be varied continuously between 21° and 42° which means a continuous, fast and flexible opening of shielding of about 42° - 84° . Together with three monochromators, Ge, bent Si and pyrolytic graphite (PG), the opening angle allows a wavelength selection between 1 \AA and 2.4 \AA . For strain measurements it is essential to set up for almost all types of materials the reflection of interest at or close to 90° in 2θ . For texture analysis one needs low index reflections. The Si monochromator is particularly well suited to strain measurements since it offers a moderate high neutron flux at the sample position as well as high resolution over a small range in scattering angle 2θ , due to the possibility to adjust the horizontal curvature of the silicon crystals for optimised focussing conditions. With the vertical focussing of Ge monochromator it is possible to get high resolution over a wider region of scattering angle which is favourable for texture measurements. The PG monochromator offers the highest neutron flux but for limited number of wavelengths and moderate resolution only used for texture measurements. Numbers and graphs for neutron flux and standard resolution functions of STRESS-SPEC have already been published elsewhere [9-11].

Besides resolution function, the instrument transparency function (pole figure window) is another essential parameter for pole figure measurements. The pole figure window is designated by the pole figure angles $\Delta\alpha$ and $\Delta\beta$, as described in detail by Moras [12]. The angle α corresponds to the latitude of the pole sphere and is a combination of the sample tilting angle χ and the diffraction angle γ (rotation angle of the base from the Debye-Scherrer diffraction cone). The longitude angle described by β represents the sample rotation ϕ . The pole figure window size $\Delta\beta$ varies with α according to equation,

$$\Delta\beta = \Delta\beta_{equator} \cdot \frac{1}{\sin(\alpha)} \quad (1)$$

The instrument transparency function of STRESS-SPEC diffractometer was examined for the Ge monochromator since it is the one most frequently used for pole figure measurements. Tab. 1 lists the pole figure window sizes close to the two limiting wavelengths of the Ge (311) monochromator. They were determined using a Si single crystal sample. The values are obtained from the equator position of the pole figure. It should be noted that the variation of monochromator curvature only affects the angle α . The variation of the pole figure window size at STRESS-SPEC for different focusing setups can also be used to correlate the instrument transparency function with texture sharpness.

The maximum usable beam diameter for global texture measurements is 25 mm. For local texture measurements the slit systems [10, 11] which are used normally for strain scanning can be utilised. The primary slit system before the sample allows to vary the incident beam size from $\emptyset = 1$ mm to $\emptyset = 25$ mm while a secondary slit can be placed in the diffracted beam. Its horizontal width is adjustable from 0 mm up to 15 mm. Gauge volumes for local texture measurements are typically in the range between $2 \times 2 \times 2$ mm³ and $5 \times 5 \times 5$ mm³ [13]. Instead of the secondary slit system a radial collimator can be put in front of the detector for even better gauge volume definition and background reduction. Two radial collimators are available at STRESS-SPEC having an FWHM of 2 mm and 5 mm, respectively.

The standard equipment for pole figure measurement at STRESS-SPEC is an Eulerian cradle type Huber 512 with asymmetric ϕ -table arrangement to gain more space for sample environment, see Fig. 1 (a). A set of standard sample holders, see for instance Fig. 1 (b) with a rock salt sample, for routine measurements and a large variety of special sample holders are available. A small xyz-stage for local texture measurement can be mounted on the ϕ -table. Due to the restricted free space inside the Eulerian cradle the sample movement is limited. As shown of the TEX-2 diffractometer at Helmholtz-Centre Geesthacht [14], a loading device of about 20 kg (20 kN load for compression / tension) can be also mounted inside such an Eulerian cradle at STRESS-SPEC.

To overcome the spatial limitation for sample manipulation and to be more flexible in strain and texture mapping a robot system based on an industrial Stäubli RX160 robot combined with a laser tracker positioning system has been developed [15, 16]. A maximum load capacity of 25 kg is possible for the robot arm. A laser tracker can be used to determine accurately the sample position using a set of reflectors mounted on the robot arm. Before the actual measurement, the movement of robot can be simulated to ensure its correct path and to avoid collisions with the optical systems of the diffractometer. A sample positioning accuracy down to 100 μ m can be achieved. Fig. 2 (a) shows the robot including a heavy basement with a total weight of about 2t on sets of air pads. On Fig. 2 (b) the set-up of a first combined stress and texture measurement on a rotary friction welded steel/aluminium sample is given. In this measurement both stress and texture in several points near the welding region along axial and radial axes were mapped without having the need to change the machine setup as in conventional instruments. In the current state this robot system is available for standard global and local texture measurements.

Furthermore, in future this robot system will open some other additional options such as to run an automatic sample changer, to offer more flexibility in the arrangement of continuous pole figure scanning, and to improve the mapping in combination with a 3D sample shape laser scanning system. The automatic sample changer is particularly necessary for measuring a large number of pole figures as shown in section 4. This sample changer is now under design and will be available in the middle of 2011.

STRESS-SPEC can be equipped with two different types of ³He area detectors, a smaller one with 200×200 mm² and a slightly larger one with 300×300 mm². By varying the detector angle a total range of 2θ between 30° and 120° can be covered. That means, related

to the wavelength range, d-values from 4.8 Å- 0.6 Å can be investigated by the larger area detector.

3. Pole figure measurement at STRESS-SPEC

Pole figure measurement by neutron diffraction is similar to standard X-ray texture diffraction to obtain the variation of diffracted intensities for about 1368~32400 sample orientations. However, due to the high penetration power of neutrons complete pole figures are obtained. For that reason neutron pole figures are of the highest quality and normalisation can be done directly by integrating over complete pole figures.

The instrument software at STRESS-SPEC supports two methods for pole figure scanning. Firstly, a step scan mode which allows running sample rotation φ in constant steps $\Delta\varphi$ from 0° to 360° , as shown in Fig. 3 (a) with a constant grid of $5^\circ \times 5^\circ$. At any tilt angle χ step width in $\Delta\varphi$ can be adapted to the texture sharpness. The area detector allows any step width in $\Delta\chi$ for data evaluation. Equal angular scans as well as equal area scans are possible. Secondly, continuous scanning along φ is implemented comparable to spiral scanning using conventional X-rays. A schematic illustration of continuous scanning method is shown in Fig. 3 (b). Continuous scanning has the advantage for eliminating positioning time and for STRESS-SPEC the total counting time can be reduced to 30%. Furthermore, continuous rotation guarantees that all crystallites contribute, which is not the case for most pole figure scanning routines in other diffractometers. Related to rotation speed and detector readout time the data storage can be accomplished with every 1° in φ rotation or as desired by the user. It should be noticed that the robot system offers more freedom to optimise the rotation speed and also to combine pole figure measurement with x, y, z scanning (texture mapping). Number of tilt positions in χ depends on the 2θ angle, the radii of the Debye-Scherrer rings and the sample to detector distance. Due to the sample composition and the sample to detector distance a number of pole figures can be measured simultaneously as shown for Mg-Al composite in Fig. 4.

A software package StressTexCalculator (STECA) has been developed which allows to extract pole figure data for intensity pole figures (crystallographic texture), for peak position pole figures (macro strain) or for peak broadening pole figures (micro strain) and to construct diffraction patterns (phase analysis) as well as strain profile patterns as function of x, y, z (strain mapping). Details and the advantages of this STECA software have been reported elsewhere [17].

4. Examples

The following examples present typical materials related to experimental needs such as single phase metals, two phase composites, minerals, local textures and the correlation of intensity pole figures with peak shift pole figures and peak broadening pole figures. In this paper we focus on the texture measurement of different types of samples and not on the texture interpretation which has been done elsewhere according to the publications.

4.1 Rolled Al7020 alloy [16]

Many applications are routine investigations of high symmetric single phase metallic samples. To perform such kind of measurements precisely in a short time is especially attractive for the users utilizing neutron diffraction. A round robin Al7020 rolled sheet was selected to compare the pole figure quality measured at STRESS-SPEC and TEX-2. The test sample was a cube of $10 \times 10 \times 10 \text{ mm}^3$ with a typical and strong deformation texture. At TEX-2 the wavelength of 1.332 Å was used. Intensities for a total of 679 points for a complete pole figure using equal area projection method were collected by a single detector. At STRESS-SPEC the Ge (311) monochromator and a wavelength of 1.22 Å was selected. Due to a sample to detector distance of 900 mm and a detector height of 200 mm in γ , a range of 20° is obtained in one detector picture. For this arrangement 5 tilt angles were necessary to cover complete pole

figures with a sufficient overlap. Intensity data were obtained by continuous scanning in ϕ with data storage at every 2° . The speed was $10 \text{ sec.}/5^\circ$ so that for the total counting time of 1.8 h, a sum of 648 detector pictures were collected, which is just 1/3 of the time consumed by TEX-2.

Fig. 5 shows Al (111) and Al (200) complete pole figures which were measured at TEX-2 and STRESS-SPEC, respectively. Both results indicate a strong rolling type texture with strong brass- $\{110\} \langle 112 \rangle$, copper- $\{112\} \langle 111 \rangle$ and S- $\{123\} \langle 634 \rangle$ components. Note that the higher pole intensity from STRESS-SPEC comes from its high resolution.

4.2 Rectangular extruded composites [4]

Multi-phase materials with special properties are attractive for extreme applications (high temperatures, high strength, extreme low density, etc.). Such materials are, among others: composites (metal-matrix composites, ceramic composites, etc.), multi-phase intermetallic compounds (Al-Ti, Al-Si, Al-Ti-Si, etc.) and ceramic materials. A complete texture analysis of a multi-phase polycrystalline material consists of the texture determination of all components of the sample. A good example of metal-metal composite is given by hot extruded 40%Vol.Mg-60%Vol.Al powder sample. Three Al reflections and eight Mg reflections were measured using four 2θ positions with Ge the (311) monochromator and a wavelength of $\lambda = 1.65 \text{ \AA}$. Total measuring time was only 6.5 h. In Fig. 6 complete measured Mg (10.0) and Mg (00.2) as well as complete measured Al (111) and Al (200) pole figures are presented. One can see on one hand the orthorhombic pole figure symmetry related to rectangular extrusion and on the other hand the superposition of a round extrusion texture with a rolling texture. The texture sharpness is related to the deformation degree and the Al/Mg ratio in the composite.

It should be pointed out that neutron diffraction is favoured for the investigation on composites particularly on metal matrix composites due to the fact that absorption can be neglected for most materials and consequently, in contraposition to X-ray diffraction, anisotropic absorption related to the microstructure (globular or lamellar) plays no role.

4.3 Textures in geological materials [18]

Neutron diffraction pole figures are characterised by high grain statistics even on coarse-grained materials which is of great advantage for geological scientific researches. Although STRESS-SPEC is not optimised for geological samples, particularly for rock-forming minerals and clays, the variety of geological samples opens many options to use it for geological texture studies. Especially, the restriction for high d -values hinders the direct investigation of basal plane pole figures of clays, chlorites and mica. With a 20 mm cubic calcite specimen an example is presented, which can be measured very easily at STRESS-SPEC. The experiment was done by the small area detector so that three 2θ positions were necessary to cover five reflections. The used wavelength was of $\lambda = 2.5 \text{ \AA}$ obtained by the Ge (311) monochromator. The total counting time for the 5 pole figures is about 17 h. A much shorter counting time, close to 50%, can be realized using the larger area detector and the PG (002) monochromator. Fig. 7 shows the (104), (006) and (110) pole figures of the calcite specimen. The texture is very well developed but very weak compared to metals. Weak textures need always longer counting time.

4.4 Texture gradient on a bonelike extrusion profile of Mg-Ze10 alloy [19]

Investigations of texture gradients or local textures in bulk samples need comparably long counting time, due to smaller gauge volumes. For texture mapping it is as important as for strain profile analysis to realize a constant gauge volume during all sample rotations and tilts. The present example is an extruded Mg Ze10 alloy with a dog-bone shape. We use a slit system of $2 \times 2 \text{ mm}^2$ to obtain on one hand sufficient local resolution and on the other hand to optimise the total counting time. Moreover, to reduce the total counting time we restrict the

set of theoretically necessary six experimental pole figures to three pole figures. Mg (10.0), (00.2) and (10.1) were obtained simultaneously with the small STRESS-SPEC area detector at one detector position. Fig. 8 shows the (10.0) and (00.2) pole figures in correspondence to three selected positions inside the dog-bone extrudate.

A texture gradient is clearly visible from central part (position 1) to the top part (position 5). This is very typical for many manufacturing processes which have an inhomogeneous materials flow or a remarkable temperature gradient during processing. That means, many crystallographic textures, particularly of engineering products, do not have only one crystallographic texture but a texture gradient. This was one of the main reasons to install the robot for handling semi-finished and industrial products.

4.5 Comparison among intensity, peak broadening and peak shift pole figures

Intensity pole figures are well established for crystallographic texture descriptions. The other two types of pole figures are still exotic mainly due to extremely long counting time and the high requirements on experiment. Only a few peak shift and peak broadening pole figures are published. High flux and high resolution instruments having a fast detector readout system opens these types of investigations. As a first example a 75% Vol. Al-25% Vol. Nb rectangular extruded bar was taken after 95% deformation degree. A cubic sample of $10 \times 10 \times 10 \text{ mm}^3$ was cut and fixed on a vanadium pin. The texture after extrusion is quite clear following the deformation behaviour of each phase, but due to co-extrusion we expect a much weaker texture than in pure metals. For peak shift we would expect no anisotropy so that a random texture should result but whether the micro strain correlates with the crystallographic texture is under discussion. The measurement was carried out with the Ge (311) monochromator and a wavelength of 1.67 \AA . Due to the overlap of Al (111) with Nb (110), these two reflections cannot be used. The counting statistic was fixed by a standard texture measurement not by a higher counting statistic for peak shift or peak broadening measurements. Data analysis to extract all three types of pole figures is possible by STECA [17].

The result for Al (200) is shown in Fig. 9. (1) The crystallographic texture was as expected. (2) The peak broadening pole figure shows the orthorhombic sample symmetry and clear structure. (3) A random peak shift pole figure which indicates no strain anisotropy inside the sample cube. (4) A remarkable similarity between Al (220) intensity pole figure and Al (200) peak broadening pole figure is observed. However, to make an interpretation of this result one needs additional experiments to exclude experimental errors and to verify this correlation.

5. Summary

STRESS-SPEC is a high flux materials science neutron diffractometer having a flexible instrument setup suitable for fast global and local texture measurements. Moreover, crystallographic texture analysis can be combined with micro- and macro-strain. Meanwhile, a wide spectrum of materials can be investigated. Looking at the main advantage of neutrons, the high penetration power, new developments will concentrate firstly on shortening the total counting time (detector development, fast adjustment, sample changer) for global texture measurements of sets of industrial samples and secondly on the implementation of the robot system RX160 for texture and strain mapping of industrial components. It is essential to combine high efficient measurements with a user friendly and fast data evaluation, available in house at STRESS-SPEC by the STECA program package.

This instrument is now available for routine operation and open for both national and international users.

Acknowledgements

We thank U. Garbe, P. Spalthoff, G. Seidl, B. Schwebke for taking part on instrumental or software developments as well as supporting some experiments.

References

- [1] D. Banabic, H.-J. Bunge, K. Pöhlandt, A.E. Tekkaya, Formability of Metallic Materials, Springer Verlag, Berlin-Heidelberg, 2000.
- [2] H.-R. Wenk, P. Von Houtte, Rep. Prog. Phys. 67 (2004) 1367-1428.
- [3] H.-G. Brokmeier, Mater. Sci. Forum. 408-412 (2002) 149-154.
- [4] H.-G. Brokmeier, Textures & Microstr. 10 (1989) 325-346.
- [5] J. Chadwick, Proc. Roy. Soc. A136 (1932) 692-708.
- [6] B. N. Brockhouse, Can. J. Phys. 31 (1953) 339-355.
- [7] G. E. Bacon, Neutron Diffraction, third ed., Clarendon Press, Oxford, 1975.
- [8] H. J. Bunge, Mathematische Methoden der Texturanalyse (Akademieverlag), 1969, Berlin.
- [9] Hofmann, G.A. Seidl, J. Rebelo-Kornmeier, U. Garbe, R. Schneider, R.C. Wimpory, U. Wasmuth, U. Noster, Mater. Sci. Forum. 524-525 (2006) 211-216.
- [10] M. Hofmann, J. Rebelo-Kornmeier, U. Garbe, R. C. Wimpory, J. Repper; G. A. Seidl, H. G. Brokmeier, R. Schneider, Neutron News, 18 (2007) 27-30.
- [11] M. Hofmann, J. Rebelo-Kornmeier, U. Garbe, R. C. Wimpory, J. Repper; G. A. Seidl, H. G. Brokmeier, R. Schneider, Physica B385-389 (2006) 1035-1037.
- [12] K. Moras, A. H. Fischer, H. Klein, H. J. Bunge, J. Appl. Cryst. 33 (2000) 1162-1174.
- [13] U. Garbe, M. Hofmann, H.-G. Brokmeier, Z. Kristallogr. Suppl. 26 (2007) 171-176.
- [14] H.-G. Brokmeier, Physica B, 234-236 (1997) 1144-1145.
- [15] J. Rebelo-Kornmeier, M. Hofmann, U. Garbe, C. Randau, J. Repper, A. Ostermann, W. Tekouo, G.A. Seidl, R.C. Wimpory, Advances in X-Ray Analysis. 52 (2009) 209-216.
- [16] H.-G. Brokmeier, C. Randau, W. Tekouo, M. Hofmann, W. Gan, M. Müller, A. Schreyer W. Petry, Mater. Sci. Forum. 652 (2010) 197-201.
- [17] C. Randau, U. Garbe, H.-G. Brokmeier, J. Appl. Cryst. 2011 (accepted).
- [18] H.J. Bunge, W. Skrotzki, S. Siegesmund, K. Weber, Textures of Geological Materials, DGM-Verlag, Oberursel (1994) 327.
- [19] H.-G. Brokmeier, C. Randau, U. Garbe, P. Spalhoff, J. Bohlen, Proce. 8th Inter. Conf. on Mg Alloys & their Applications, Weimar Germany, (2009) 583-588.

Figure captions

Fig. 1 (a) Eulerian cradle with a Cu-sample mounted on the asymmetric ϕ -table; (b) rock-salt sample mounted on a standard sample holder.

Fig. 2 (a) Robot RX160 mounted on a heavy basement; (b) RFW steel/aluminium sample on robot for stress and local texture measurements.

Fig. 3 Schemes of pole figure scan with (a) discrete method using an equal angular $5^\circ \times 5^\circ$ and (b) with discrete steps in χ ($0 \sim 90^\circ$) and continuous scanning of ϕ ($0 \sim 360^\circ$).

Fig. 4 (a) Detector image of an Mg/Al composite including Mg (10.0), Mg (00.2), Mg (10.1); (b) Diffraction pattern related to Fig. 4 (a).

Fig. 5 Measured Al (111) and (200) pole figures at TEX-2 and STRESS-SPEC, respectively.

Fig. 6 (a) Measured Mg (10.0) and (00.2) pole figures; and (b) Measured Al (111) and (200) pole figures.

Fig. 7 Three measured complete pole figures (104), (006) and (110) of a calcite specimen.

Fig. 8 Dog-bone extrudate with marked measurement points and Mg (10.0) and Mg (00.2) pole figures corresponding to positions 1, 3 and 5.

Fig. 9 Comparison of peak intensity, peak broadening and peak position pole figure of Al (200) from a 75%Vol.Al-25%Vol.Nb rectangular extruded bar.

Table captions

Tab. 1 Pole figure window size at STRESS-SPEC.

Fig. 1

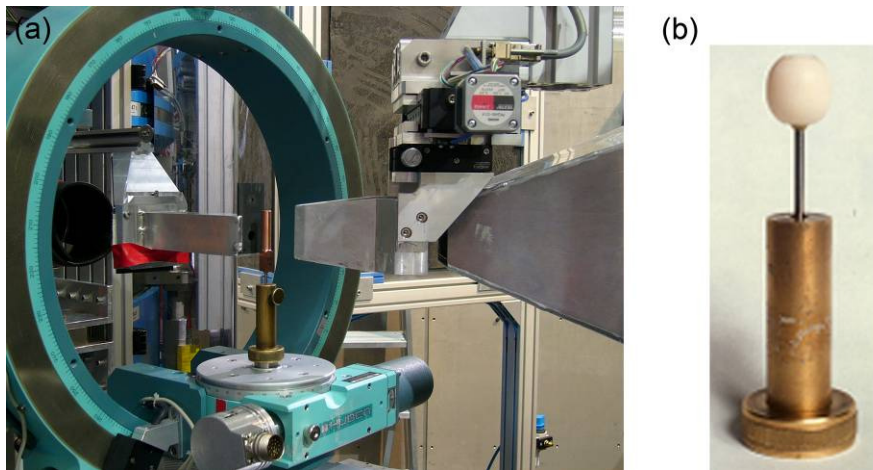


Fig. 2



Fig. 3

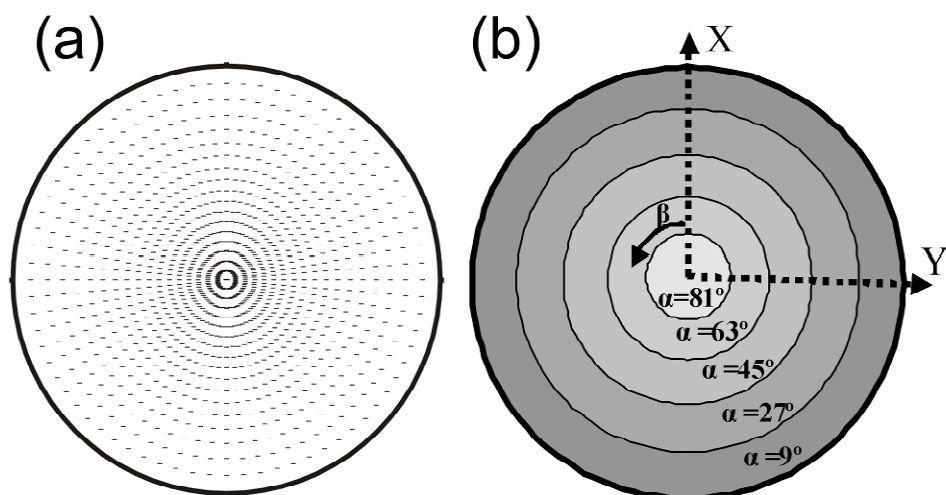


Fig. 4

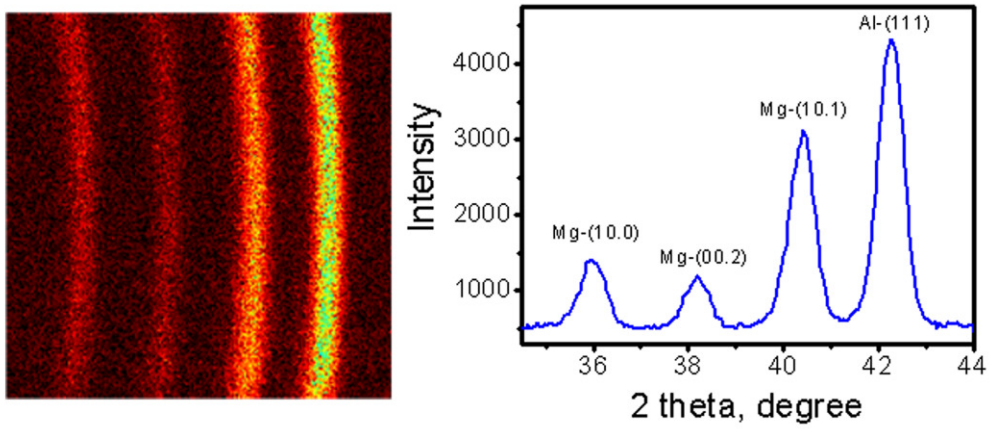


Fig. 5

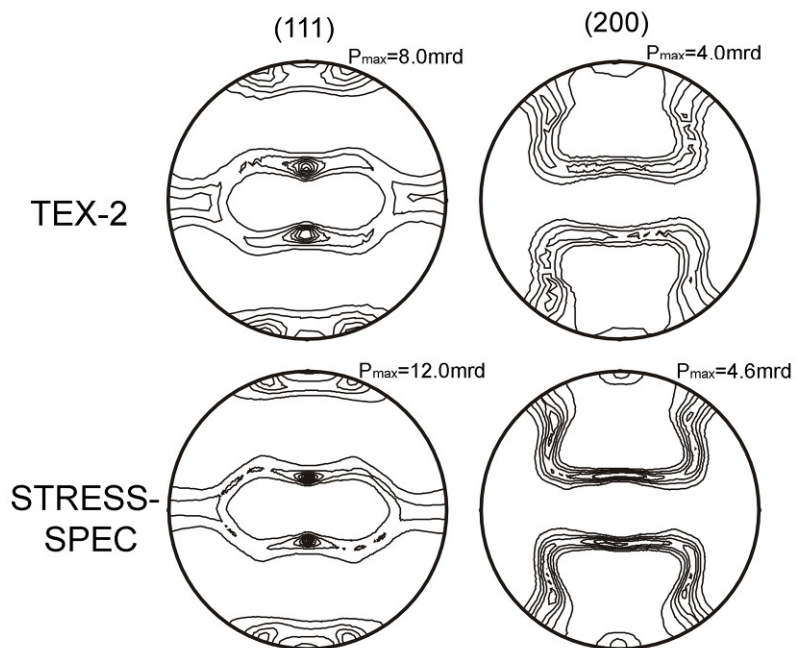


Fig. 6

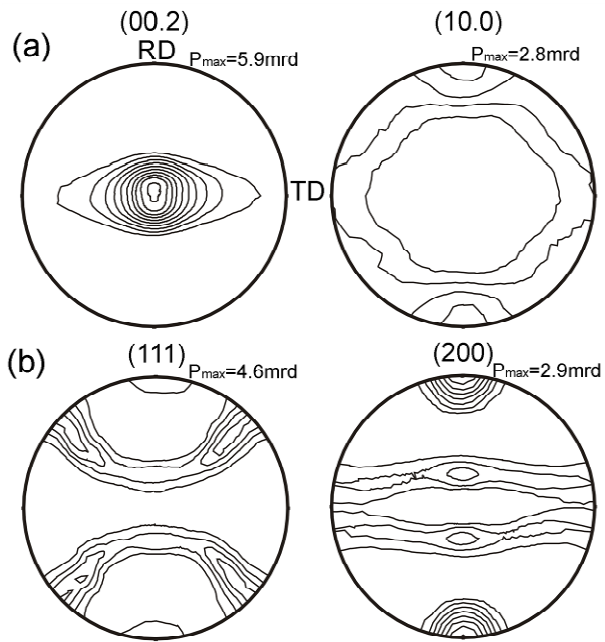


Fig. 7

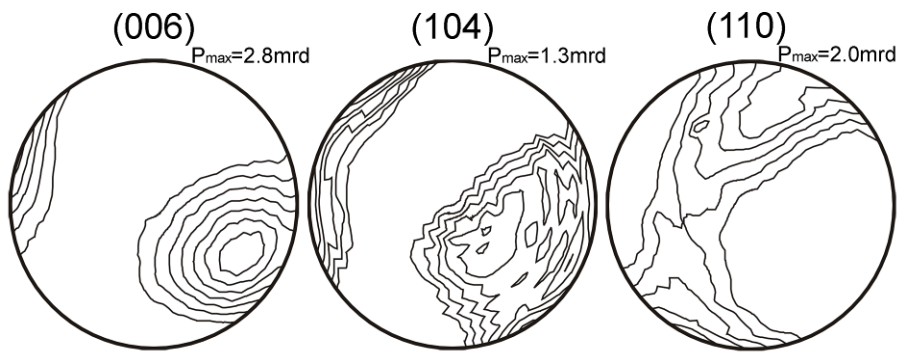


Fig. 8

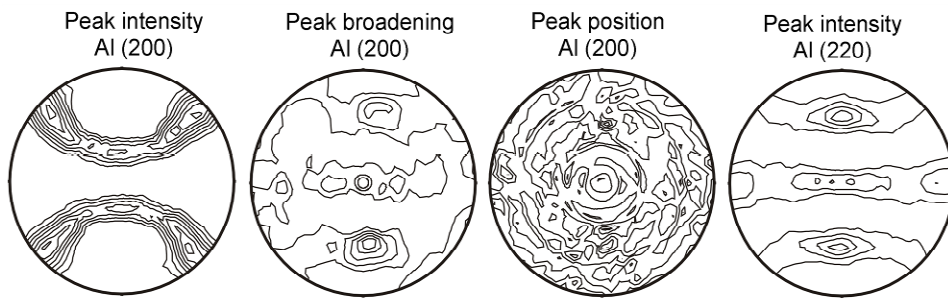
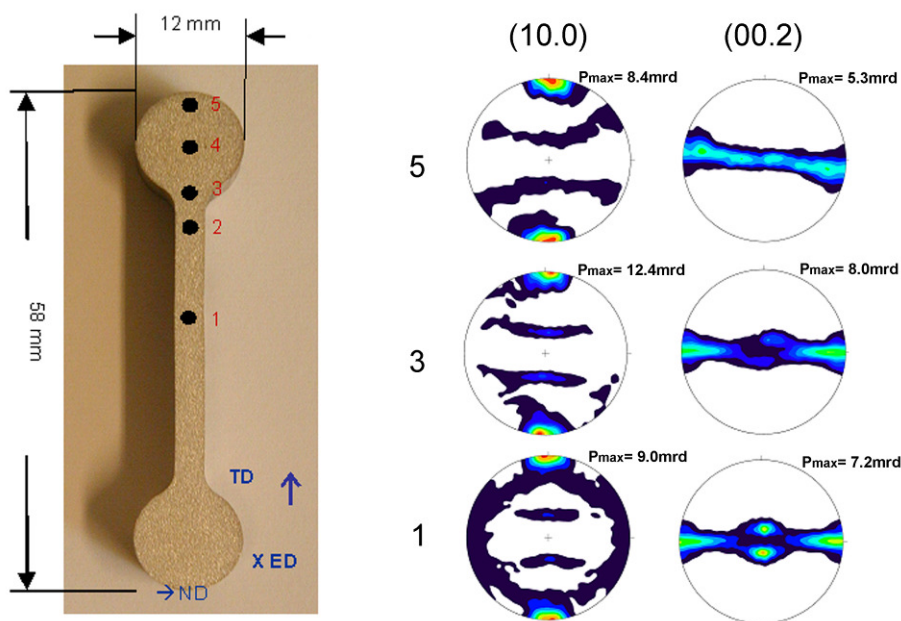


Fig. 9



Tab. 1

Wavelength, Å	Focus	$2\theta, ^\circ$	$\Delta \alpha, ^\circ$	$\Delta \beta_{equator}, ^\circ$
1.22	yes	55	2.32	0.34
1.22	no	55	1.20	0.36
1.76	yes	82	1.68	0.35
1.76	no	82	0.74	0.34